Top applications of dermatologic ultrasonography that can modify management

ULTRA SONO GRAPHY

Ximena Wortsman[1,2,3]

[1]Institute for Diagnostic Imaging and Research of the Skin and Soft Tissues, Santiago;
[2]Department of Dermatology, Faculty of Medicine, Universidad de Chile, Santiago;
[3]Department of Dermatology, School of Medicine, Pontificia Universidad Catolica de Chile, Santiago, Chile

REVIEW ARTICLE

https://doi.org/10.14366/usg.22130
eISSN: 2288-5943
Ultrasonography 2023;42:183-202

Dermatologic ultrasonography is a new field that has been growing exponentially in the last 10 years. It has multiple applications that can modify patient management, such as the assessment of benign and malignant cutaneous tumors, vascular anomalies, inflammatory dermatologic entities, aesthetic complications, and nail lesions. Compared with other imaging techniques such as computed tomography or magnetic resonance imaging, ultrasonography has the highest axial spatial resolution and has benefited from the development of high- and ultra-high-frequency probes that could even reach 70 MHz. The daily use of ultrasonography in dermatology has been reported to improve the accuracy of diagnoses, the tracking of activity, and the assessment of severity in common dermatologic conditions, which certainly can support better treatment of patients.

Keywords: Ultrasonography; Dermatology; Skin; Cancer; Hidradenitis suppurativa

Key points: Ultrasonography supports the modification of the management of common dermatologic conditions by enabling an early diagnosis, activity tracking, and severity assessment. The main applications of dermatologic ultrasonography include benign and malignant cutaneous tumors, vascular anomalies, inflammatory dermatologic entities, aesthetic complications, and nail lesions.

Received: July 31, 2022
Revised: September 20, 2022
Accepted: October 5, 2022

Correspondence to:
Ximena Wortsman, MD, Institute for Diagnostic Imaging and Research of the Skin and Soft Tissues; Department of Dermatology, Faculty of Medicine, Universidad de Chile; Department of Dermatology, School of Medicine, Pontificia Universidad Catolica de Chile, Lo Fontecilla 201 of 734, Las Condes, Santiago 7591018, Chile
Tel. +56-222446058
Fax. +56-222446058
E-mail: xworts@yahoo.com

Introduction

The use of dermatologic ultrasonography has significantly increased in the last decade. This mainly seems to be the result of technological advances, such as the increase in the frequency of probes and a growing number of publications on the topic [1]. To date, the dermatologic applications of ultrasonography include benign and malignant skin tumors, vascular anomalies, cutaneous inflammatory conditions, aesthetic procedures, and nail lesions [2–8].

Moreover, published guidelines for performing examinations allow standardization of the procedure and, therefore, its quality [2,8]. These guidelines recommend that a physician performs and interprets the examinations. A minimum of 300 examinations per year is considered to assess competence,

How to cite this article:
Wortsman X. Top applications of dermatologic ultrasonography that can modify management. Ultrasonography. 2023 Apr;42(2):183-202.

and the recommendations include using color Doppler ultrasound devices with multifrequency probes operating at a frequency ≥15 MHz [8]. Multiple options that even reach 70 MHz are now available on the market.

The axial spatial resolution of high-frequency ultrasonography is much higher than that of magnetic resonance imaging (MRI) and computed tomography (CT). This means that ultrasonography can discriminate patterns in submillimeter structures. In contrast, MRI and CT need structures that measure ≥3–5 mm to discriminate a tissue pattern. The axial spatial resolution of ultrasonography is 100 microns at 18 MHz and 30 microns at 70 MHz, which is comparable to lower degrees of magnification on histology [1,9].

The success of any imaging technique in the real-world practice of medicine relies on the capacity to modify the diagnosis and/or treatment. Dermatology is no exception to this statement. Therefore, in this review, we will focus on the applications where ultrasonography can indeed generate a change in the management of patients.

The images presented in this manuscript were obtained following the principles of medical ethics of Helsinki, and the patients provided signed informed consent for the publication of their images.

Basic Anatomical Concepts

On ultrasonography, the "epidermis" presents as a hyperechoic line, except in the palmar and plantar regions, where it usually manifests as a bilaminar and thicker hyperechoic layer. The keratin content mainly provides the echogenicity of the epidermis, and its presence is higher in the palms and soles, explaining its appearance in these sites.

The "dermis" manifests as a hyperechoic band less bright than the epidermis, and its echogenicity is primarily given by the collagen content. The dermis varies in thickness according to the site on the body; for example, it is thinner in the face and ventral forearms and thicker in the dorsal and lumbar regions. A hypoechoic band located in the upper dermis is usually detected in photoaging, which occurs in sun-exposed areas of the skin. This is called the subepidermal low echogenicity band, and should not be confused with inflammatory conditions.

The "hypodermis," also called subcutaneous tissue or subcutis, presents as a hypoechoic layer, and its echogenicity is given by the fatty tissue. Between hypoechoic fatty lobules, there are hyperechoic linear structures that correspond to fibrous septa (Fig. 1) [10,11].

The "nail unit" comprises the nail plate, the nail bed, and the periungual skin. The nail plate presents as a hyperechoic bilaminar structure with a dorsal and ventral aspect. The nail bed appears as a hypoechoic space. The matrix region is in the proximal part of the nail bed, where usually the echogenicity of the nail bed slightly increases. The periungual skin is divided into the proximal nail fold, the lateral periungual regions, and the hyponychium. The periungual skin lacks fatty tissue and presents epidermis and dermis (Fig. 2) [10–13].

The "hair follicles" manifest as oblique or straight hypoechoic dermal bands. The "hair tracts" can present as trilaminar or bilaminar hyperechoic structures (Figs. 1, 3). Most of the scalp hair is trilaminar, and the bilaminar hair tracts, also called villus hairs, are present in the scalp to a greater extent than in the rest of the body [10,11,14]. The predominance of villus (bilaminar) over trilaminar hair tracts in the scalp has been reported in certain types of alopecia, such as androgenetic alopecia [15].

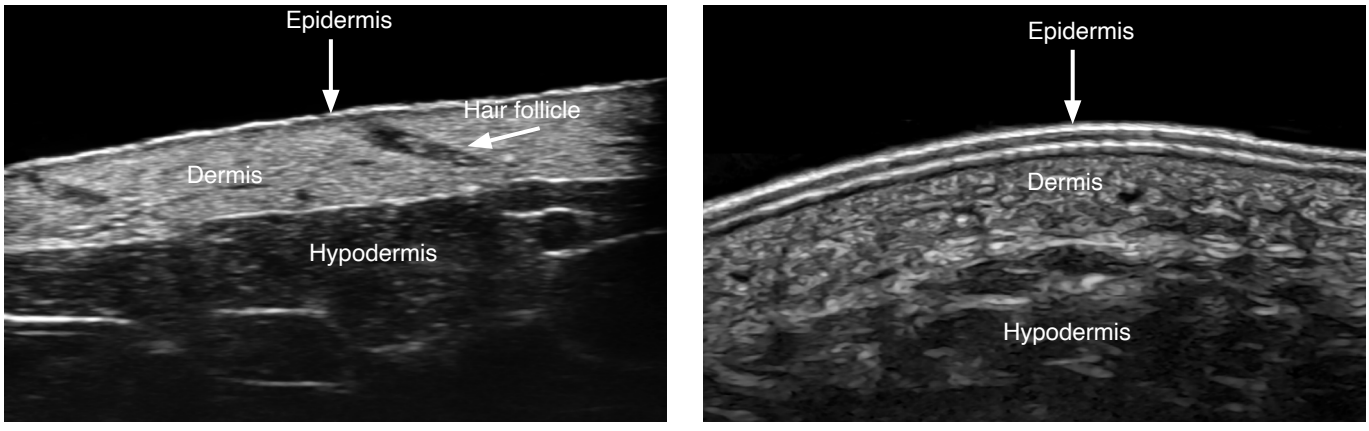

A B

Fig. 1. Normal ultrasound anatomy of the skin.
These images (A, forearm skin at 70 MHZ; B, plantar skin at 24 MHz) present the ultrasonographic patterns of the epidermis, dermis and hypodermis at different frequencies. Notice the echostructure of the hair follicle in A.

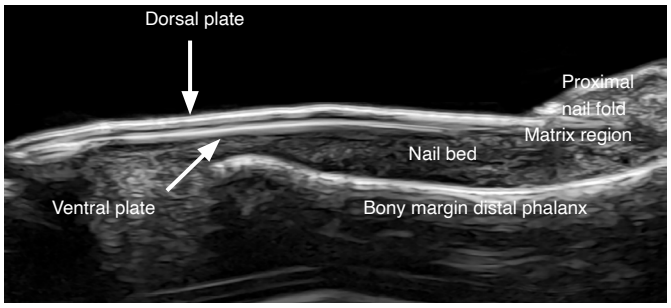

Fig. 2. **Normal ultrasound anatomy of the nail (longitudinal view; index finger) at 24 MHz.** The vertical arrow shows the dorsal plate and the oblique arrow presents the ventral plate.

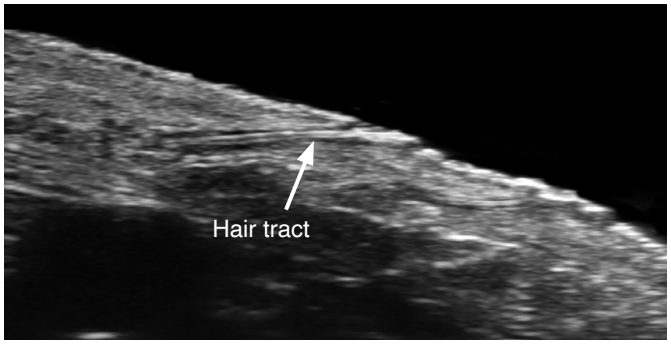

Fig. 3. **Normal hair tract (arrow) within a dermal hair follicle before emerging into the surface at 70 MHz.**

On color Doppler, it is possible to detect low-velocity vessels (≤15 cm/s) with arterial and venous blood flow in the subcutaneous tissue and very few vessels in the dermis. This is due to the current sensitivity of machines, which can usually detect flow ≥2 cm/s; therefore, currently, the blood flow within the normal dermal vessels is difficult to detect on ultrasonography [10,11].

Technical Considerations

The requisites for dermatologic ultrasonography examinations include color Doppler ultrasound devices operated with linear or compact linear high-frequency probes (≥15 MHz) and a trained operator. Books, articles, and courses now include dermatologic ultrasonography in their programs, some of them under the umbrella of well-known scientific organizations such as the American Institute of Ultrasound in Medicine (AIUM; http://www.aium.org) and the European Federation of Societies in Ultrasound and Biology (EFSUMB; http://www.efsumb.org), among others.

Regarding the technique, it is recommended to use a copious amount of gel on the surface of the skin and nails and not to compress the cutaneous vessels. To stabilize the hand in the gel, it is possible to use the fifth finger. The protocol includes a sweep in grayscale in at least two perpendicular axes, color Doppler or power Doppler, and a pulsed Doppler (spectral curve) analysis. This scheme makes it possible to discriminate the tissue patterns, the main vascularity features, distinguish arterial from venous flow, including arteriovenous shunts, and detect the blood flow velocity.

The limitations of dermatologic ultrasonography include the detection of lesions that measure <0.1 mm at 15 MHz and <0.03 mm at 70 MHz, epidermal-only lesions, and identifying pigments such as melanin [10,11,16].

Main Dermatologic Conditions

In these entities, ultrasonographic information provides relevant anatomical data that cannot be deduced from a dermatologic clinical examination. This includes the nature (solid or cystic), the exact size, and location of a lesion or lesions, the layers involved, a vascular versus non-vascular appearance, the type and velocity of the vascularity, active versus inactive lesions in inflammatory conditions, and benign versus malignant appearances, among other features.

Benign Cutaneous Tumors and Pseudotumors

Multiple tumors and pseudotumors can be studied using ultrasonography. Among the most frequent are the following:

Epidermal cyst

These are composed of remnants of epidermal components in the dermis and/or hypodermis and present a granular layer. These cysts contain keratin and cholesterol crystals and commonly discharge a cheesy yellowish material. Under inflammation, the cyst suddenly increases in size and may rupture internally within the skin. The treatment of epidermal cysts is usually surgical and preferably when the cysts are intact; therefore, it is important to know in advance if the cyst is intact or ruptured. Moreover, it should be determined whether there are remnants of the cyst capsule after a rupture because this means that the cyst will tend to recur over time. Thus, if a ruptured cyst undergoes surgery, this capsule remnant should be removed.

On ultrasonography, a cyst's appearance may vary according to its phase. If a cyst is intact, it can show a round or oval shape, hypoechoic or anechoic, but mostly hypoechoic, dermal, and/or hypodermal structure. In 20% of cases, there is a communicating tract to the subepidermal or epidermal layer called a punctum. Sometimes the cyst presents an oval shape with multiple anechoic bands that correspond to cholesterol crystals that may occasionally resemble a testicle, a presentation called a "pseudotestes" appearance.

When a cyst is inflamed, it increases in diameter and becomes more heterogeneous. During partial rupture, the hypoechoic keratin is spread into the neighboring tissues generating inflammation, and some of the borders become irregular.

In total rupture, there is an internal burst of the cyst, and all the keratin is spread into the vicinity and sometimes extrudes outside the skin. The cyst becomes totally irregular, hypoechoic, and sometimes heterogeneous.

A posterior acoustic enhancement artifact is commonly conserved in all these stages, which may help identify an epidermal cyst.

Using 70 MHz, it is usually possible to identify remnants of the capsule of the cyst; however, in some cases, at 18 or 24 MHz, it is feasible to detect remnants of inflamed fragments of the capsule. The capsule appears as a thin and slightly echogenic layer when the cyst is intact, while in conditions of inflammation, it presents as a hypoechoic band.

On color Doppler, there is a variable degree of vascularity with slow-flow vessels according to the degree of inflammation in the periphery of the cyst. In the total rupture phase, some vessels may be found within the remnant of the cyst due to inflammation and granulation tissue (Fig. 4) [10,11,16–28].

Pilomatrixoma

Pilomatrixoma is a hair matrix-derived benign tumor commonly found in children. Clinically, it has been reported to be misdiagnosed in up to 56% of cases. Thus, it can be clinically mistaken for an epidermal cyst or other benign tumors, including vascular lesions [1,10,11,26,27,29].

On ultrasonography, the most frequent form of presentation is the target type with a hypoechoic rim and a hyperechoic border that contains hyperechoic spots that correspond to calcium deposits. The detection of calcium is the key sign for diagnosing this tumor (Fig. 5). Other forms of presentation are the heterogeneous and the mixed-echogenicity (anechoic and hypoechoic) forms [1,10,11,18,26,27,30–37].

Mixed-echogenicity pilomatrixoma is also called cystic or bullous pilomatrixoma, and its appearance is usually caused by internal bleeding. The latter form of presentation may be tricky clinically because it is softer on palpation than the usual pilomatrixoma. The cause of the internal bleeding can be trauma and/or inflammation, and it may also present internal hypoechoic septa [10,11,36].

On color Doppler, the vascularity varies and can range from hypovascular to hypervascular. The hypervascular form of pilomatrixoma can be clinically mistaken for vascular lesions such as infantile hemangiomas. This is important because pilomatrixomas are commonly removed surgically, whereas infantile hemangiomas are treated with medication such as propranolol or timolol [10,11,31,36].

Dermatofibroma

This benign fibrous tumor has several variants, and the most common form of presentation is the nodular type. Other rarer variants include the aneurysmal, hemosiderotic, and atrophic subtypes. Clinically, a frequent presentation is an erythematous and firm nodule in the extremities or the trunk, which may be mistaken for an epidermal cyst or a pilomatrixoma.

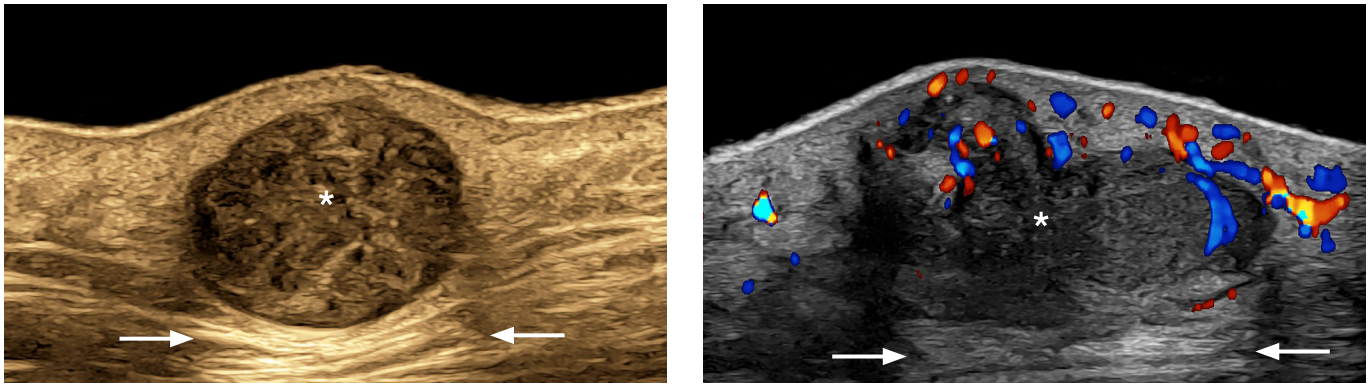

A B

Fig. 4. Epidermal cyst (24 MHz).
A. Intact (left cheek): grayscale ultrasonography with a color filter presents a well-defined, round-shaped, hypoechoic dermal and hypodermal structure (*). Posterior acoustic enhancement is noted at the bottom of the cyst (arrows). B. Ruptured (right dorsal forearm): color Doppler ultrasonography presents a partially lobulated hypoechoic dermal and hypodermal structure with some ill-defined areas at the bottom and a more intense hypoechoic band on the surface suggestive of a fragment of the capsule. The cyst generates a posterior acoustic enhancement artifact at the bottom (arrows). The hypervascularity in the periphery of the cyst should be noticed. There is also increased echogenicity of the surrounding hypodermis due to inflammation.

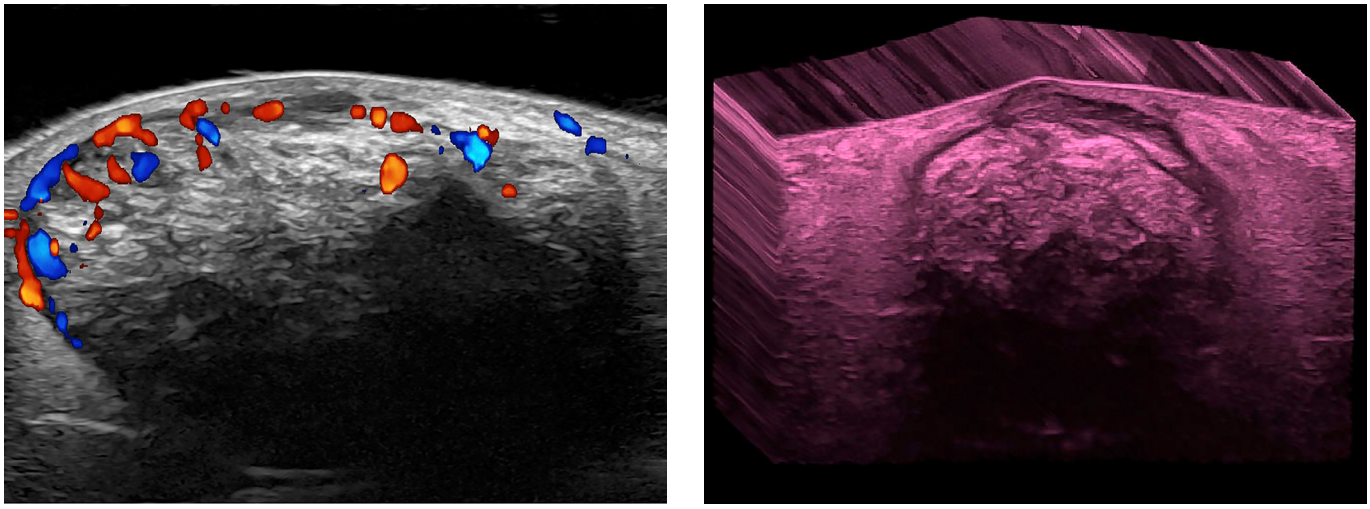

A B

Fig. 5. Pilomatrixoma of the "target type" (24 MHz; right arm).
Color Doppler (A) and three-dimensional grayscale reconstruction with a color filter (B) show a well-defined, oval-shaped dermal and hypodermal structure. There are multiple hyperechoic focal areas suggestive of calcifications, some of them with posterior acoustic shadowing artifact. On color Doppler, there is hypervascularity in the periphery of the tumor.

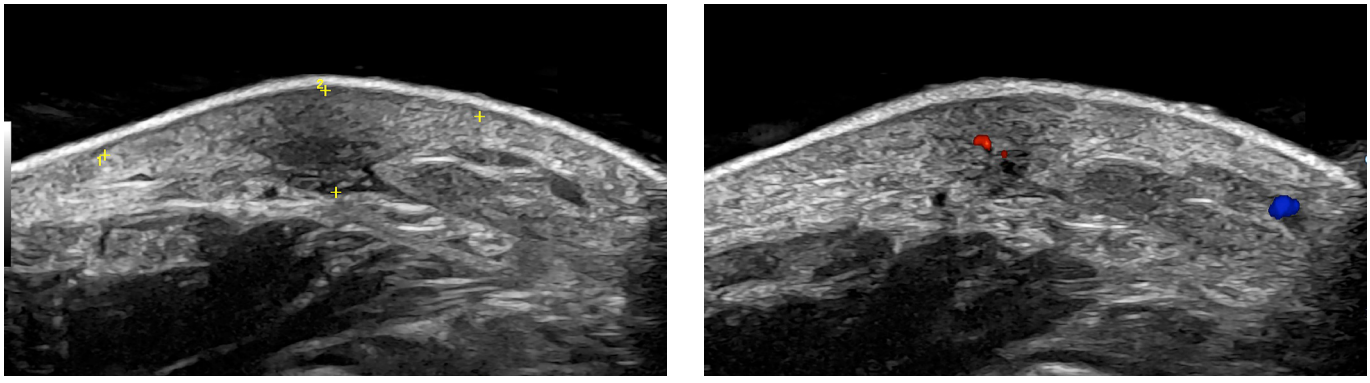

A B

Fig. 6. Dermatofibroma.
Grayscale (A) and color Doppler ultrasound (B) images (24 MHz; dorsum of the right foot) present hypoechoic ill-defined dermal focal zone (between markers), slightly fusiform, with a more deeply hypoechoic central part. On color Doppler, there are few vessels within the structure.

On ultrasonography, the nodular type shows an ill-defined hypoechoic focal dermal zone that may protrude into the hypodermis and displace the epidermis upward. This focal area commonly shows an even more intense hypoechoic center and distortion of the regional hair follicles. On color Doppler, they present no or a low degree of vascularity with low-velocity vessels (Fig. 6).

In contrast with dermatofibrosarcoma protruberans (a malignant type of fibromatous tumor), dermatofibromas do not show hyperechoic pseudopods in the hypodermis, and the fatty tissue is compressible with the probe [11,38].

Skin Cancer

The main objectives of using ultrasonography in skin cancer include the need to detect the extent of the tumor, including depth, the involvement of deeper layers, and the main vessels or structures close to the tumor. This supports the selection of the type of surgery (e.g., standard vs. Mohs) or a non-surgical treatment (e.g., topical, cryosurgery, etc.) according to the characteristics of each tumor. Ultrasonography is also a useful tool for performing locoregional staging. More accurate anatomical information could improve the results of oncologic treatment and the cosmetic appearance of the patient, allowing a one-time procedure with proper free margins [38–40].

Importantly, this information is impossible to obtain from a clinical examination, although it is critical for surgical planning. This is a tremendous advantage compared to other imaging techniques used in dermatology, such as dermoscopy, confocal microscopy, and optical coherence tomography, which are limited by their superficial penetration lower than 2 mm.

In comparison with CT and MRI, ultrasonography is the only imaging technique that enables detection of the primary tumor [6,38–48].

Non-melanoma skin cancer

Non-melanoma skin cancer (NMSC) is the most common cancer in humans. It can be divided into basal cell carcinoma (BCC) and squamous cell carcinoma (SCC). The BCC is the most common subtype. NMSC is frequently found in regions exposed to the sun, such as the face.

On ultrasonography, BCC usually appears as an oval, band-like, or irregular hypoechoic dermal and/or hypodermal structure that usually presents hyperechoic spots (Fig. 7). However, variable shapes have been reported in the literature. The number of hyperechoic spots has been linked to the tumor's aggressiveness. Thus, it has been reported that ≥7 hyperechoic spots within the tumor suggest a high risk of recurrence, corresponding to histologic subtypes such as micronodular, infiltrative, morpheaform, and metatypical. The hyperechoic spots are believed to correspond to compact nests of atypical cells besides some calcifications and corneum cysts.

SCC presents as a hypoechoic or irregular dermal and/or hypodermal structure that does not show hyperechoic spots. SCC is more aggressive than BCC and usually requires locoregional staging because it may present regional metastasis, albeit with lower frequency than melanoma (Fig. 8).

On color Doppler, the vascularity is variable, but tends to be lower in BCC than SCC and with low-velocity vessels. However, some cases of BCC and SCC may present prominent vascularity.

Melanoma

Melanoma is the most lethal skin tumor but, fortunately, the least common. Melanomas are usually hyperpigmented lesions; however, there are amelanotic variants that have hidden pigment.

On ultrasonography, melanoma presents as a hypoechoic dermal and/or hypodermal lesion that may extend to deeper layers. The depth of melanoma is of paramount importance because it

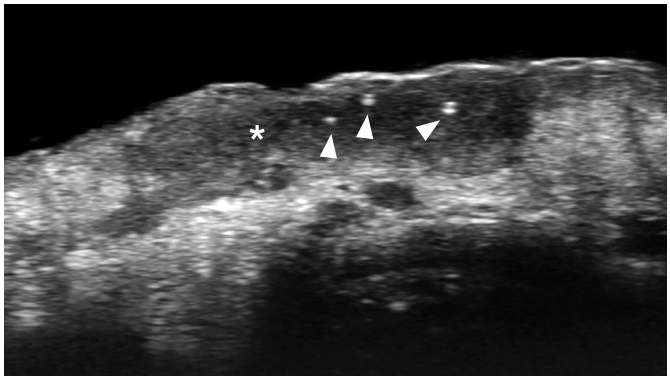

Fig. 7. **Basal cell carcinoma (low risk of recurrence; macronodular type; 70 MHz; nasal tip).** Ultrasonography (grayscale) presents a hypoechoic dermal lesion (*) with irregular borders and a few hyperechoic spots (arrowheads).

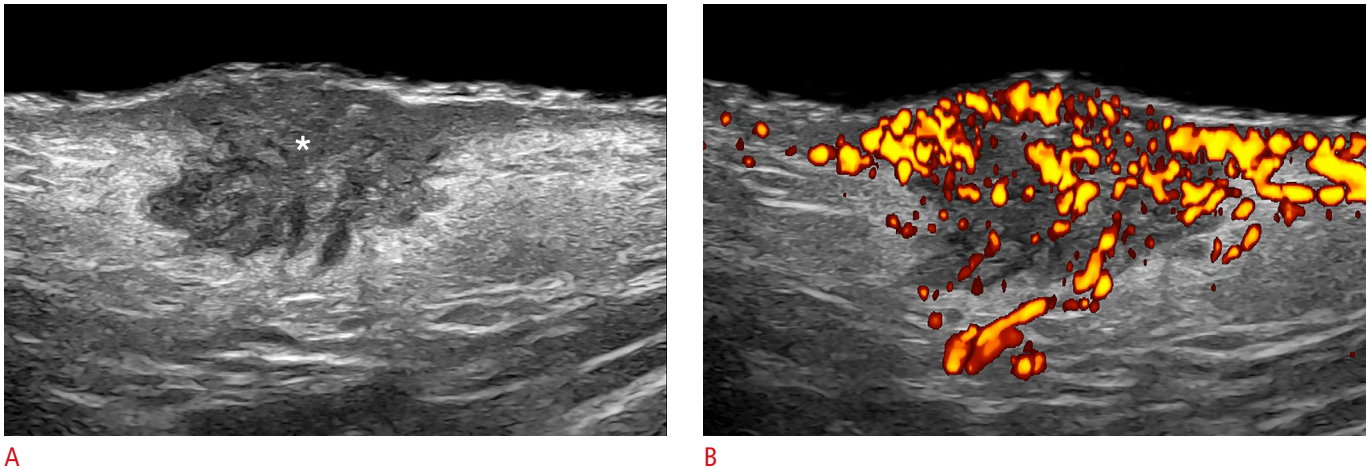

A B

Fig. 8. **Squamous cell carcinoma (24 MHz; left cheek).**
Grayscale (A) and power Doppler (B) show a hypoechoic lesion (*) with irregular borders located in the dermis and upper hypodermis. There is an upward displacement of the epidermis and increased echogenicity of the surrounding hypodermis. On power Doppler, there is prominent hypervascularity within the lesion and its periphery.

is linked to the patient's survival rate. On ultrasonography, it is possible to detect the lesion and measure all axes, including depth (ultrasonographic Breslow index). On color Doppler, melanomas tend to be hypervascular with low- or intermediate-velocity vessels.

It is essential to perform locoregional staging of melanomas and detect satellite (≥2 cm from the primary tumor), in-transit (<2 cm from the primary tumor), and nodal metastases (Fig. 9).

Signs of malignant lymph nodes include size >1 cm (transverse axis), round shape, asymmetric cortical thickening, hypoechoic inner nodules, loss of the cortex-medulla difference of echogenicity with full hypoechogenicity, and cortical and chaotic vascularity.

Knowledge of this critical information enables well-informed management that starts with a proper treatment selection, including the decision of a sentinel node procedure [10,11,42–44,49–51].

Vascular Anomalies

Infantile hemangiomas

Infantile hemangiomas are the most common vascular cutaneous tumors of childhood and show three phases. The first phase is the proliferative stage, characterized by fast growth after birth. On ultrasonography, they manifest as a mostly ill-defined, hypoechoic, and hypervascular dermal and/or hypodermal lesion. On color and pulsed Doppler, they present arterial and venous flow and commonly arteriovenous shunts. The arterial peak systolic velocities may be high and similar to the velocity of important vessels such as the carotid or the radial arteries. The presence of medium-size afferent arteries to the tumor may slow the hemangioma regression; therefore, it is important to detect them.

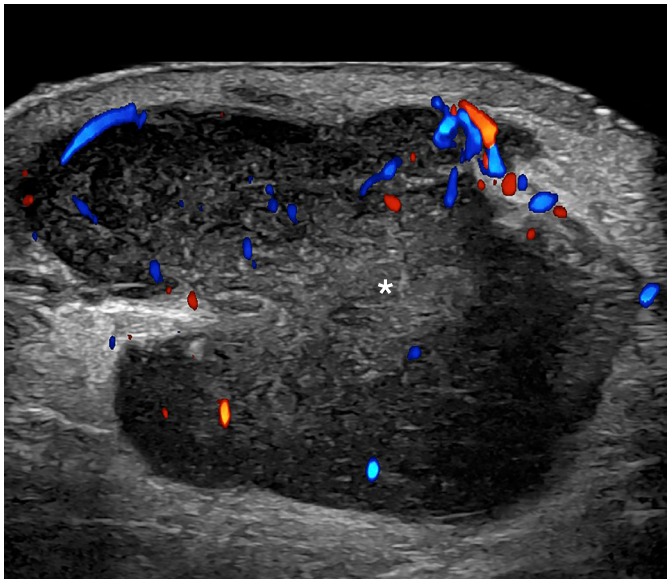

Fig. 9. Melanoma in-transit metastasis (24 MHz; right arm). Color Doppler ultrasound demonstrates a hypoechoic hypodermal nodule, slightly heterogeneous with lobulated borders and irregular vascularity. There is increased echogenicity of the surrounding hypodermis. The asterisk marks the metastasis.

The second phase is the partial regression stage, and on ultrasonography, it is characterized by a mixed echogenicity with hypoechoic and hyperechoic areas and prominent vascularity, but with a lower number and velocity of the vessels.

The third phase is the total regression phase, characterized by replacement of the vascular tissue with fibrofatty tissue. On ultrasonography, lesions in this phase tend to show a mostly hyperechoic and hypovascular appearance. Some residual low-velocity vascularity may still be present in the region.

Ultrasonography also allows detecting deeper infantile hemangiomas that involve glands or muscles. In these cases, these hemangiomas tend to be better defined, and they present the same phases of involution and, therefore, similar changes in echogenicity and the degree of vascularity.

Importantly, ultrasonography supports the diagnosis of infantile hemangioma and its follow-up; therefore, it may serve as a tool to decide the start, the type, and the treatment adjustments (Fig. 10). Thus, superficial infantile hemangiomas (only dermal) are treated differently than mixed infantile hemangiomas (i.e., involving the hypodermis and/or deeper layers). For example, superficial infantile hemangiomas are usually managed with topical timolol, and mixed hemangiomas are treated with propranolol orally.

In children with ≥5 cutaneous hemangiomas, it is crucial to study the liver because it has been reported that liver hemangiomas are more likely to be present in these patients. Furthermore, congenital syndromes with brain and spinal abnormalities should be ruled out in children with hemangiomas in the midline [1,10,11,22,23,37,52–59].

Vascular malformations

Vascular malformations (VMs) are errors of morphogenesis and not actual vascular tumors. VMs are a nest of vessels usually present at birth that show proportional growth and do not involute or disappear over time. Nevertheless, VMs may be clinically mistaken for infantile hemangiomas and vice versa, but they present a different etiology, prognosis, and management.

VMs can be classified into high-flow (arterial and arteriovenous) and low-flow (venous, capillary, and lymphatic) types. Arterial, arteriovenous, venous, and lymphatic VMs tend to present as clusters of anechoic tubules, or lacunar spaces in the dermis and/or hypodermis. To discriminate these entities, it is necessary to perform a pulsed Doppler examination (spectral curve analysis) and detect the type and velocity of the blood flow.

Arterial VMs present curves with systolic and diastolic phases.

Arteriovenous VMs show a mix of arterial and venous monophasic flow, commonly an aliasing artifact, and sometimes arteriovenous shunts with "to-and-fro" waveforms.

Venous VMs present a monophasic flow and reflux under compression with the probe. Lymphatic VMs do not show inner flow and are usually non-compressible.

Capillary VMs frequently present as changes in echogenicity without hypervascularity. Thus, when located in the dermis, they appear as hypoechoic, and in the hypodermis, as hyperechoic.

Nevertheless, mixed VMs such as venous and lymphatic or arterial and capillary are also observed.

Ultrasonography can support guided-percutaneous sclerotherapy, the decision of laser treatments, and the follow-up and/or surgical planning of VMs (Fig. 11) [6,10,11,23,27].

Inflammatory Conditions

Hidradenitis suppurativa

Hidradenitis suppurativa (HS) is a devasting autoimmune disease that affects the hair follicle. It commonly generates inflammatory lesions in the intertriginous areas, such as the axillary, groin, and gluteal regions, besides other less commonly affected areas such as the scalp, face, umbilical, inframammary, and intermammary regions,

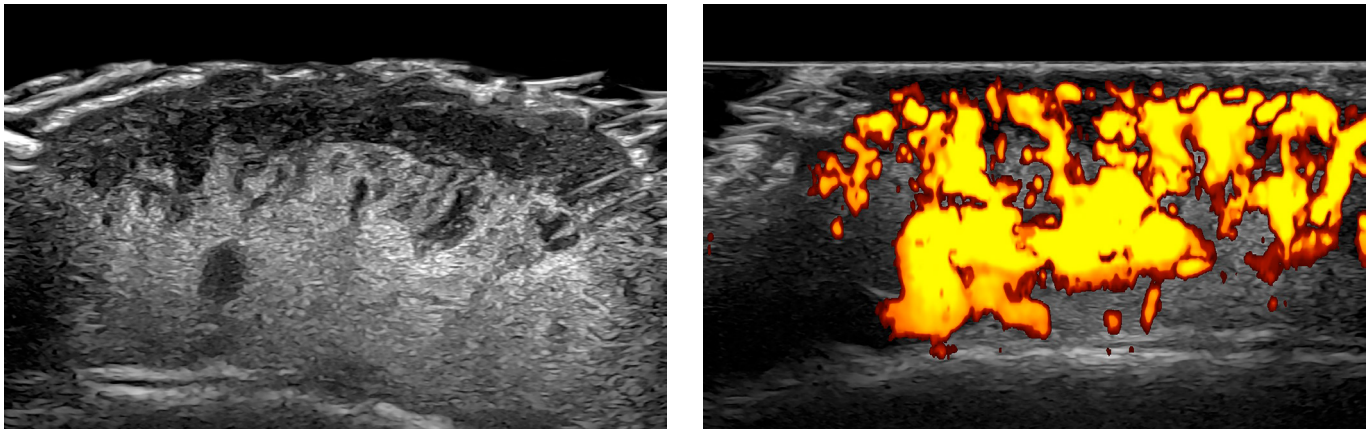

A B

Fig. 10. Infantile hemangioma in the partial regression phase (24 MHz; scalp).
A, B. Heterogeneous dermal and hypodermal mass that presents hypoechoic and hyperechoic areas. On power Doppler (B), there is prominent vascularity in the mass.

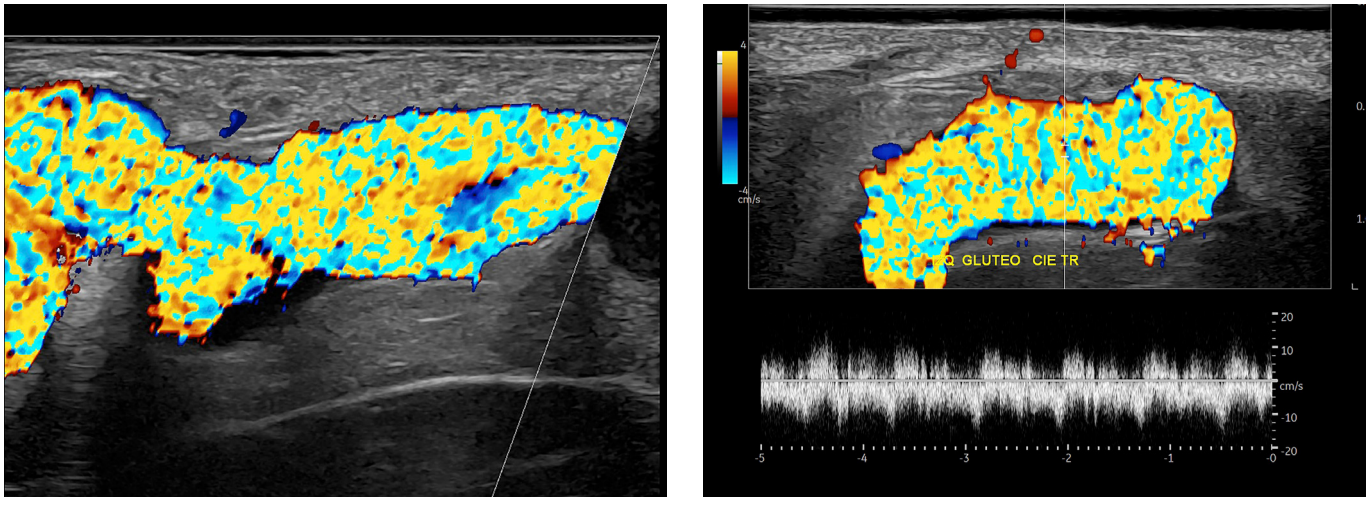

A B

Fig. 11. Arteriovenous vascular malformation (24 MHz; left gluteal region).
Color Doppler (A) and pulsed Doppler (B) show a tortuous vascular hypodermal structure with turbulent flow (aliasing artifact). The pulsed Doppler (spectral curve analysis) demonstrated a to-and-fro blood flow.

among others [60,61].

It has been widely reported that clinical scoring systems usually underestimate the severity of the disease. This is relevant because the treatment is decided according to the degree of severity of the disease. Ultrasonography supports its diagnosis, staging, and management. Moreover, it has been suggested that ultrasonography could be a standard of care in HS patients to correct the clinical staging, and it has recently been incorporated in guidelines for managing HS [62–66].

The ultrasonographic criteria for diagnosing HS include widening of the hair follicles, decreased echogenicity and thickening of the dermis, pseudocysts (hypoechoic or anechoic dermal and/or subcutaneous structures that measure <1 cm), the presence of inflammatory fluid hypoechoic collections (sac-like) and fistulous tracts, also called tunnels (band-like), that can involve the dermis and/or hypodermis [1,10,65].

Unlike other types of fluid collections and fistulous tracts, HS fluid collections and fistulas communicate to the dilated base of the hair follicles. Hyperechoic bilaminar fragments of hair tracts have been commonly reported within the HS lesions [1,10,11,27,65,67–88].

Pilonidal cysts are supposed to correspond to a localized variant of HS, since they are not actual cystic lesions and present similar sac-like or band-like, dermal, and/or hypodermal structures that contain multiple fragments of hair tracts [81].

On color Doppler, there are variable degrees of hypervascularity according to the level of inflammation. It is possible to track the activity of the disease by monitoring the hypervascularity (number, thickness, type, and velocity of the vessels) [80,84].

The most common staging system used in HS is SOS-HS, which counts the main key lesions, such as fluid collections and tunnels, and has three levels of severity [65]. Tunnels can be classified according to the degree of fibrosis and edema, their layer of involvement (dermal and/or hypodermal), or their complexity (non-communicating or communicating). This information is relevant because tunnels presenting a higher degree of fibrosis, hypodermal location, and communicating with other tunnels in the same region are less responsive to systemic treatment and commonly require surgery. The presence of hypodermal involvement and fragments of

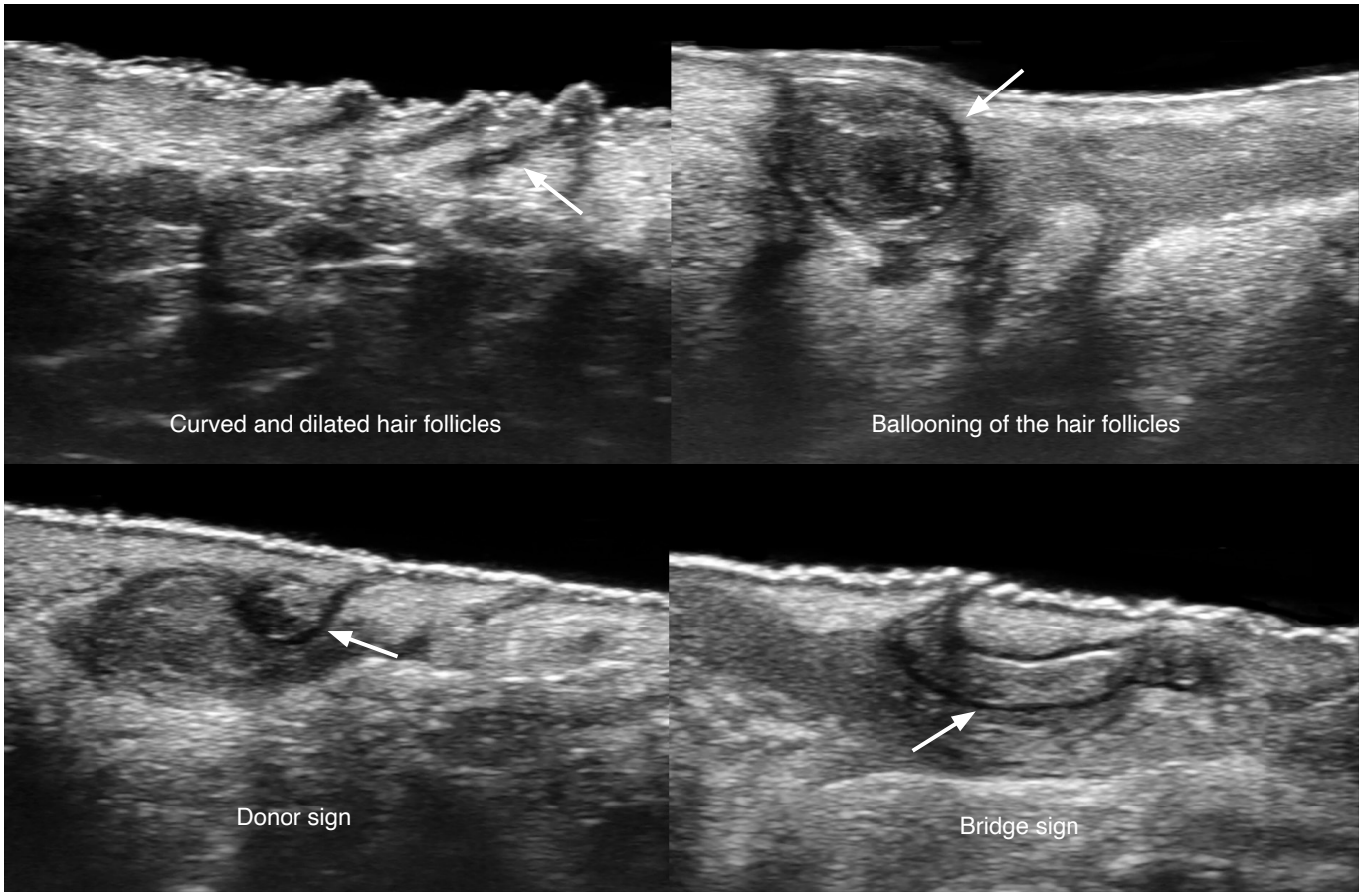

Fig. 12. **Ultrasonographic signs of early hidradenitis suppurativa at 70 MHz (axillary and groin regions).** The arrows on the left show the donor sign and the arrow on the right demonstrates the bridge sign.

hair tracts within the lesions seems to be linked to a higher severity and a perpetuation of inflammation in the disease [11,38,65,74,85].

Early signs of HS can be observed with ultra-high-frequency devices (70 MHz). These include the presence of curved, dilated, and ballooned hair follicles, hypoechoic thick bands of keratin retained in the dermis, usually connecting dilated follicular ostia (bridge sign), and pseudocysts that present fragments of hair tracts that protrude towards the neighboring dermis (sword sign) [79].

Since there is subclinical involvement in HS and a need to stage the severity of the disease, it is recommended to include in the ultrasound study all the affected regions in a bilateral way. This anatomical information is critical for the disease's medical and surgical management (Figs. 12, 13).

Morphea

This is a connective tissue disease that affects the skin (i.e., a cutaneous form of scleroderma). To date, there is no laboratory test for tracking morphea activity, which makes clinical management difficult. Notably, ultrasonography can support detection of the activity of the disease, as well as its diagnosis.

The ultrasound activity signs include echogenicity and thickness alterations of the dermis and hypodermis, loss of the definition of the dermal-hypodermal border, increased echogenicity of the hypodermis, and hypervascularity of the dermis and/or hypodermis [1,10,11,26,89].

The most sensitive signs for detecting activity in morphea are the loss of the definition of the dermal-hypodermal border, increased echogenicity of the hypodermis, and the presence of dermal and/or hypodermal hypervascularity [1,10,11,26,89].

Morphea appears differently according to the phase of the disease. In active phases, there is thickening and decreased echogenicity of the dermis with increased echogenicity of the hypodermis, as well as cutaneous hypervascularity (dermal and/or hypodermal). However, in the atrophic phase, it is possible to

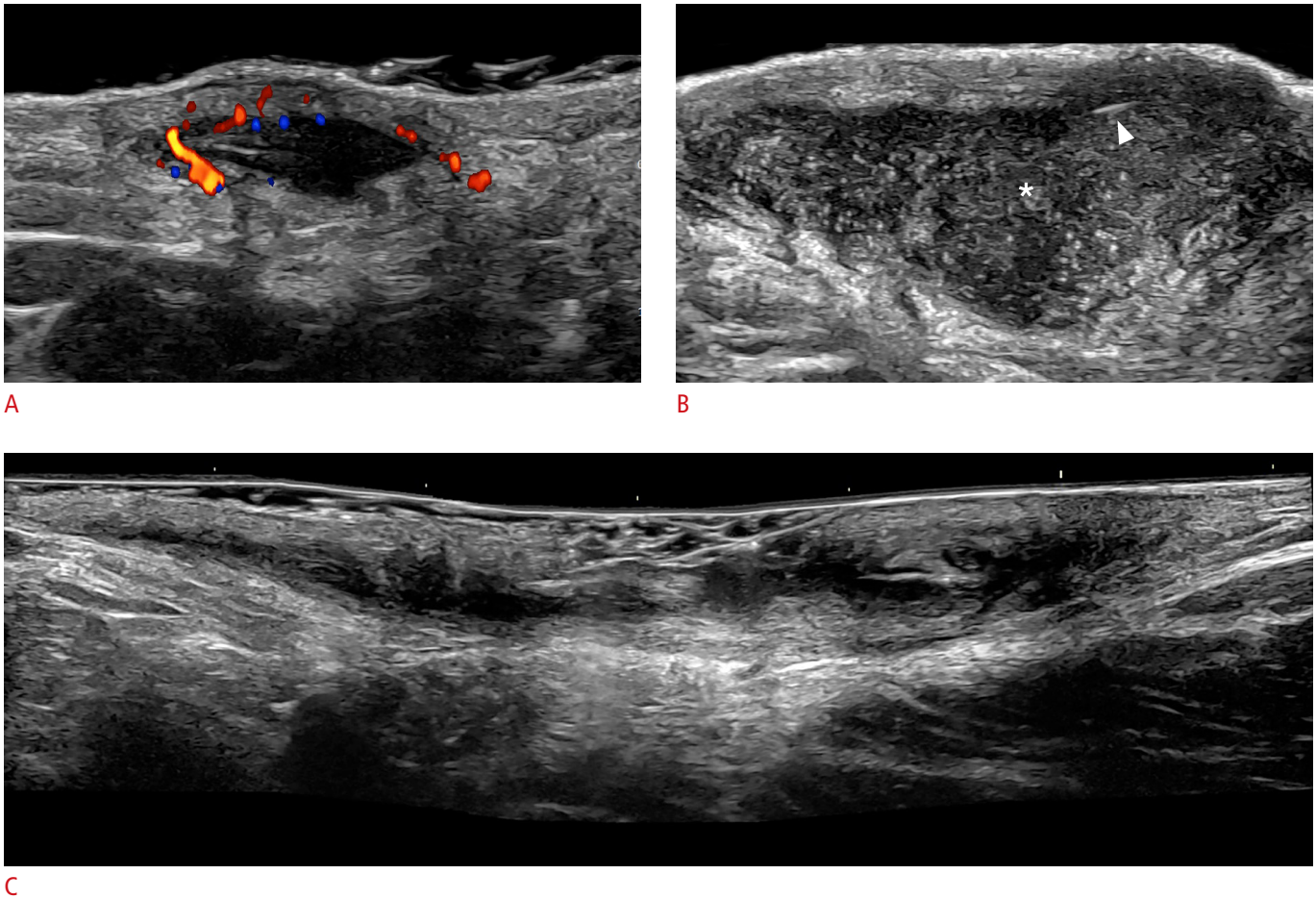

A B C

Fig. 13. Key ultrasound lesions of hidradenitis suppurativa (24 MHz; axillary and groin regions).
Pseudocyst (color Doppler) (A), fluid collection (*) (B), and fistulous tract, also called tunnel (grayscale) (C) are shown. The hypervascularity in the periphery of the pseudocyst in A and the presence of fragments of hair tracts in the fluid collection (B, arrowhead) should be noted. The pseudocyst is in the dermis, and the fluid collection and tunnel are located in the dermis and upper hypodermis.

find decreased dermal and hypodermal thickness with the loss of subcutaneous fat.

Atrophy is not a synonym for inactivity, because inflammation can still be present in the borders, the center of the lesion, and even in the adjacent regions.

Moreover, in morphea, it is common to find subclinical activity, which makes performing the examination critical for properly managing the disease; therefore, the recommended protocols include the study of the adjacent regions besides the affected corporal region. Hence, it is recommended that an ultrasound study can scan all the corporal segments, and not just the areas with visible plaque or macules (Fig. 14) [1,10,11,26,89–95].

A scoring system for assessing the degree of activity of morphea has recently been reported. This score is called US-MAS, and it can determine the basal and the follow-up degree of activity through the measurement of grayscale and color Doppler parameters [96].

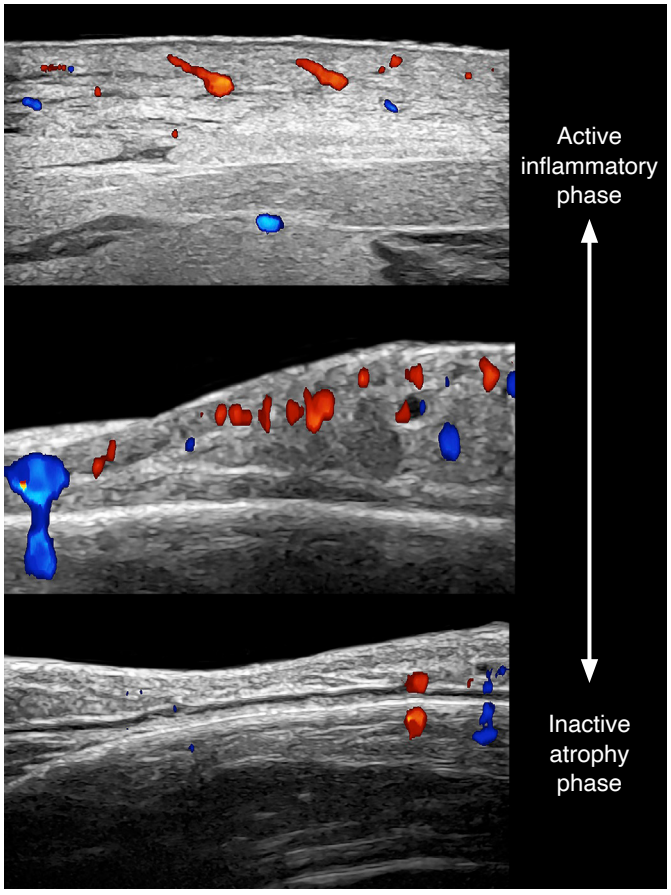

Fig. 14. Morphea (i.e., cutaneous form of scleroderma; 24 MHz; top, right breast; middle and bottom, frontal part of the face). Color Doppler ultrasound images demonstrate the different phases of activity of morphea from active (top) to inactive and atrophy (bottom).

Aesthetics

Cosmetic fillers

Cosmetic fillers are exogenous components used for treating wrinkles and sagging skin or performing an augmentation in certain corporal regions. In the last 20 years, non-surgical procedures, including cosmetic fillers, have presented explosive growth; however, most of these injections are performed blindly by different physicians (and sometimes non-medical personnel), at different institutions, sometimes in different cities and even in other countries. Furthermore, patients do not always remember the number or types of procedures performed on them. Therefore, the clinical history is commonly non-reliable, although this information would be

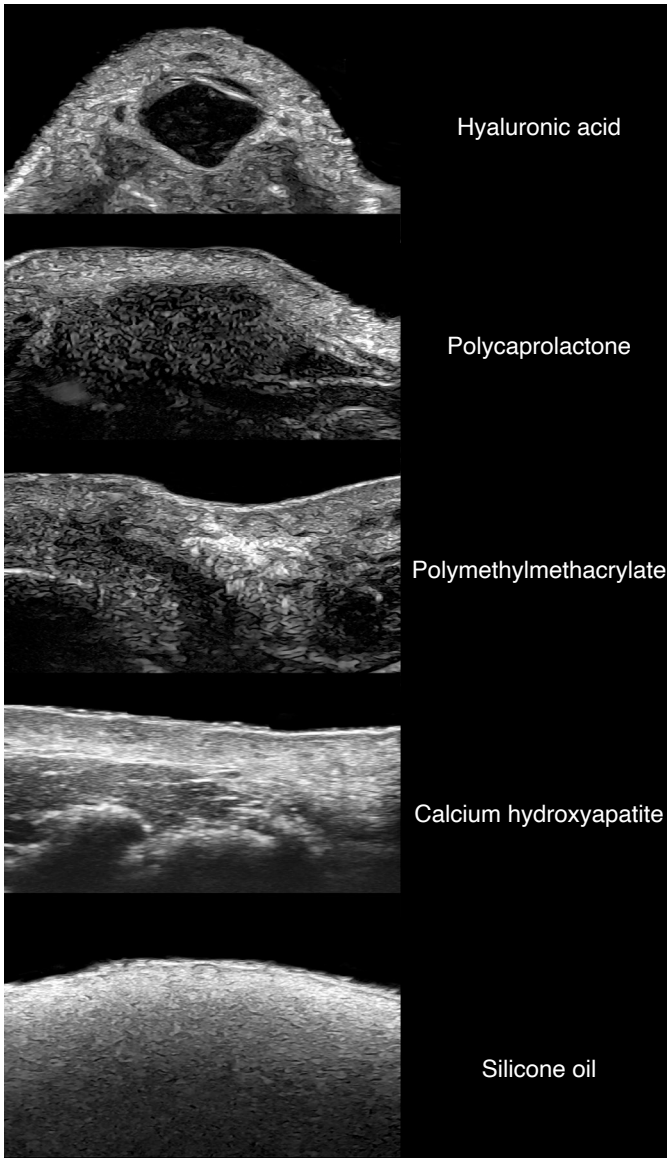

Fig. 15. Ultrasonographic patterns of common cosmetic fillers (24 MHz; facial region).

critical for planning a new cosmetic procedure or diagnosing and managing a complication that can even simulate other dermatologic conditions.

To date, ultrasonography is the only imaging modality that allows the detection and identification of the most frequently used cosmetic fillers (Fig. 15). This is done through the detection of the main patterns of the fillers and their artifacts [10,11,97–105].

Ultrasonography supports the diagnosis of early (<4 months) and late (≥4 months) complications. Early complications include vascular occlusions, hematomas, abscesses, overfilling, misplaced injections, and inflammatory reactions. Among the frequent late complications are transitory episodes of inflammation and/or edema, granulomas, and panniculitis [1,6,10,11,101].

Granulomas appear as hypoechoic dermal, hypodermal, and/or musculoaponeurotic nodules. They can present at the sites of injection and sometimes as an autoimmune sarcoidal reaction that generates multiple granulomas in areas of recent and previous procedures (Fig. 16) [1,6,10,11,101].

Panniculitis is inflammation of the hypodermis, which could appear at the site or distant from the injection site as a result of an autoimmune or infectious reaction. This shows an increased echogenicity of the hypodermis and may be classified as mostly lobular (without septal involvement), mostly septal (with septal thickening and hypoechogenicity), and mixed [10,25,101,106–108].

Secondary inflammation of the lacrimal, parotid, and submandibular glands has also been commonly observed in users of cosmetic fillers. Therefore, the ultrasound protocol for studying cosmetic fillers in the face is suggested to include all these glands [109].

Ultrasonography can support the guided injection of a filler by providing a map of the main vessels and structures and, therefore, minimizing the risk of vascular occlusion and misplacement of the filler. Additionally, ultrasonography can guide percutaneous treatments in cases with complications such as the use of hyaluronidase and steroids [97].

Nail Conditions

These include benign and malignant tumors, pseudotumors, inflammatory conditions, and location or growth alterations. Biopsies of the nail are commonly avoided because they can leave permanent scarring in the matrix; thus, the possibility of identifying the type of lesion by imaging is of great help to clinicians. On ultrasonography, it is possible to distinguish whether a lesion originates in the nail or the periungual region, its nature (solid or cystic), its exact diameter and location (e.g., proximal, intermediate, distal, central or eccentric, etc.), the degree of vascularity, and a benign or malignant appearance, which can be critical for planning the treatment. We will discuss some of the most common requests for ultrasound examinations.

Glomus tumor

Glomus tumors are benign tumors derived from the neuromyoarterial plexus, and their most common location is the nail bed. Clinically, they usually present with exquisite pain and dystrophic ungual changes.

On ultrasonography, it is possible to detect the tumor as an oval-shaped, well-defined hypoechoic nodule that commonly generates scalloping of the bony margin of the distal phalanx. According to the size and location of the tumor, it may involve the matrix region and cause alterations and upward displacement of the nail plate.

Their most common location is the proximal part of the nail bed; however, other locations, such as the middle or distal part of the nail bed, have also been observed. Glomus tumors tend to be centrally located, but they can also be eccentrically located in the nail bed.

On color Doppler, these tumors frequently present hypervascularity with low flow vessels (Fig. 17). Nevertheless, there are some hypovascular variants of glomus tumors, such as the glomangiomyoma histological subtype. Thus, the anatomical information from ultrasonography can benefit surgical planning. Moreover, it has been reported that glomus tumors with presurgical ultrasonography present lower rates of recurrence than those not previously studied

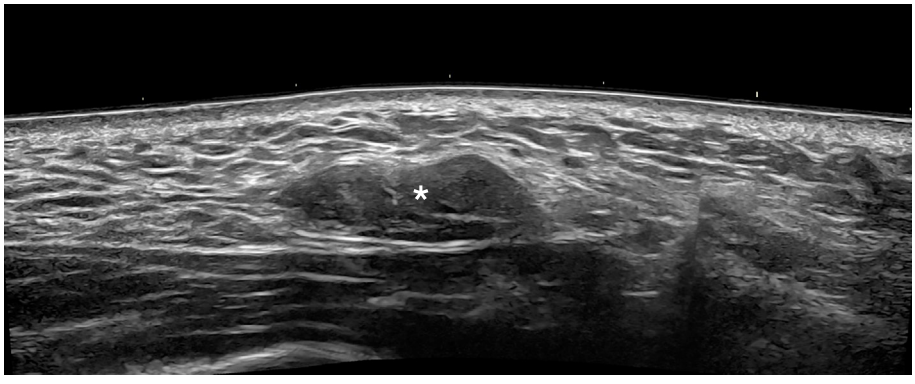

Fig. 16. **Granuloma after the injection of hyaluronic acid in the right cheek (24 MHz).** Ultrasonography (grayscale; transverse panoramic view) presents an oval-shaped and slightly lobulated nodule (*) in the hypodermis. This site was previously injected with hyaluronic acid.

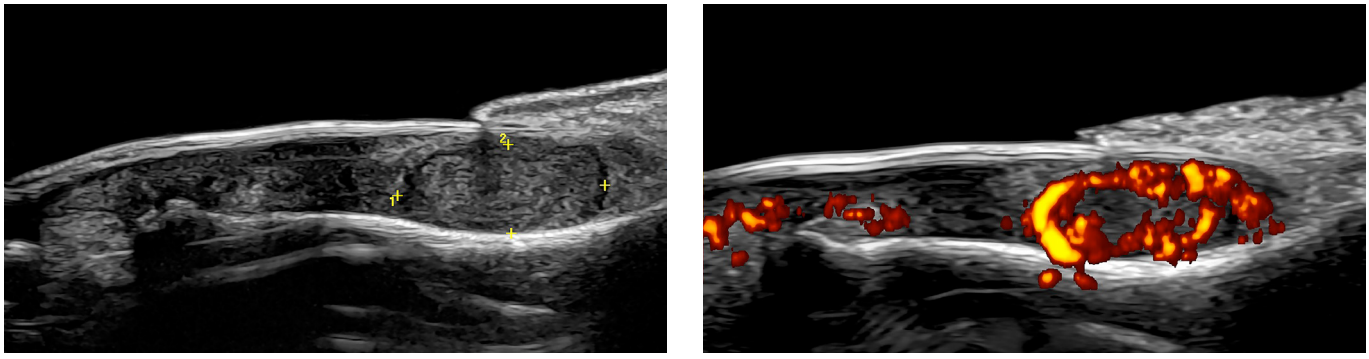

A B

Fig. 17. Glomus tumor of the nail (24 MHz; left thumb).
Grayscale (A) and Power Doppler (B) images show an oval-shaped, well-defined, hypoechoic nodule (between markers in A) in the proximal part of the nail bed. There is a slight upward displacement of the nail plate and scalloping of the underlying bony margin of the distal phalanx. On power Doppler, there is prominent vascularity within the nodule.

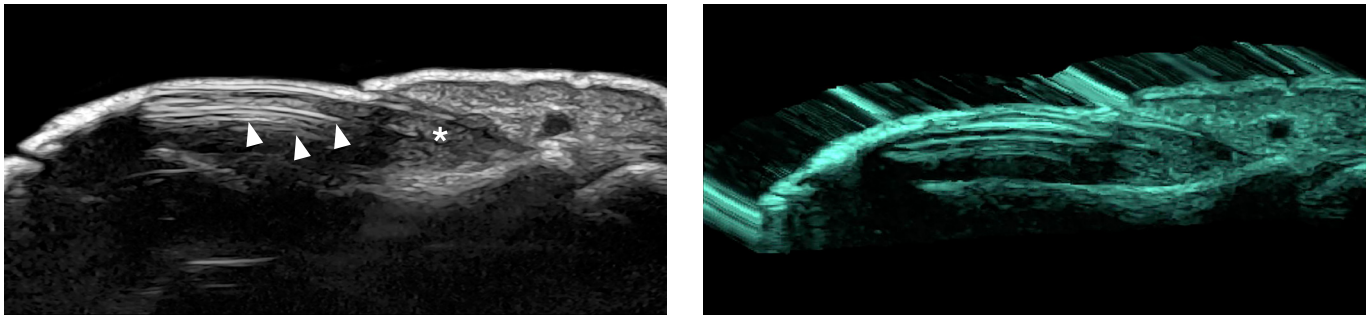

A B

Fig. 18. Onychomatricoma (24 MHz, right index finger).
Grayscale (A) and three-dimensional reconstruction (B) of the nail (with a color filter) show an ill-defined, hypoechoic structure (*) in the proximal nail bed that presents multiple hyperechoic lines protruding into the nail plate (arrowheads).

[10–13,110–116].

Onychomatricoma

Onychomatricoma is a benign tumor derived from the nail matrix that commonly generates a yellowish band in the nail plate; however, some hyperpigmented variants can clinically simulate melanoma. This tumor may also be clinically confused with other causes of onychodystrophy.

Ultrasonography can support the diagnosis and management because onychomatricoma has a pathognomonic appearance that shows an ill-defined eccentric hypoechoic subungual tumor with hyperechoic lines or spots that protrude into the nail plate.

On color Doppler, the vascularity varies and may range from hypovascular to an intermediate degree of vascularity with slow-flow vessels (Fig. 18) [1,13,116–118].

Myxoid synovial cyst

Myxoid synovial cyst is a periungual cyst originating in the distal interphalangeal joint that is commonly associated with osteoarthrosis. The cyst protrudes into the dermis of the proximal nail fold and is commonly connected to the joint through a tortuous tract. It is important to detect the connection of the cyst to the joint because it should be sealed during surgery; otherwise, the cyst will tend to recur.

On ultrasonography, it presents as oval-shaped anechoic structures located in the proximal nail fold, sometimes with lobulated borders. These cysts can generate an extrinsic compression of the proximal part of the nail plate and the area of the matrix, which usually produces a concavity and irregularities of the nail plate on the same axis of the cyst. The connecting tract to the joint appears as a tortuous anechoic duct that could go through the dorsum or the lateral borders of the joint.

On color Doppler, the vascularity is variable and ranges from

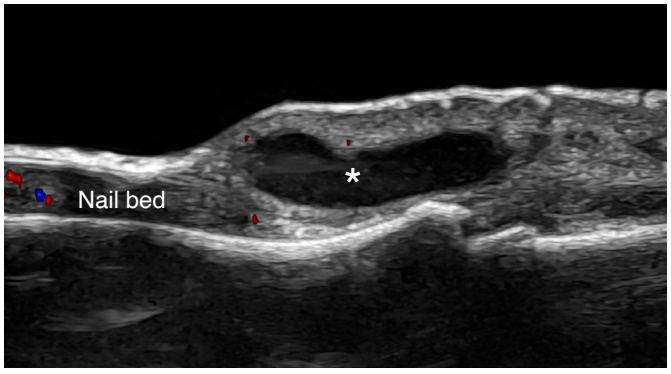

A

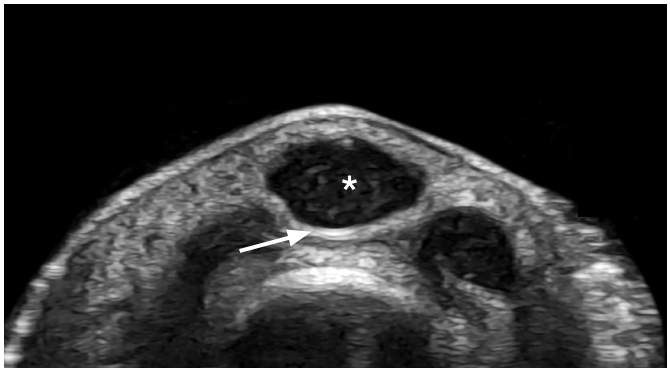

B

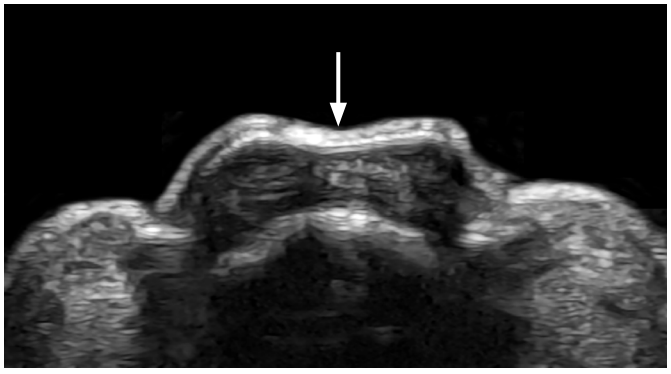

C

Fig. 19. Periungual myxoid (synovial) cyst (24 MHz; left middle finger).
Ultrasound grayscale images (longitudinal [A] and transverse view of the proximal nail fold [B], transverse view of the middle of the nail [C]) demonstrate an oval-shaped, well-defined anechoic cystic structure (*) that is compressing the proximal part of the nail plate (arrows) and therefore, the matrix region. There is a concavity in the nail plate (C) on the same axis of the cyst.

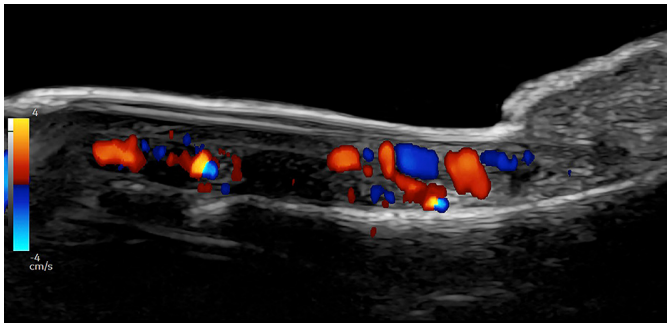

A

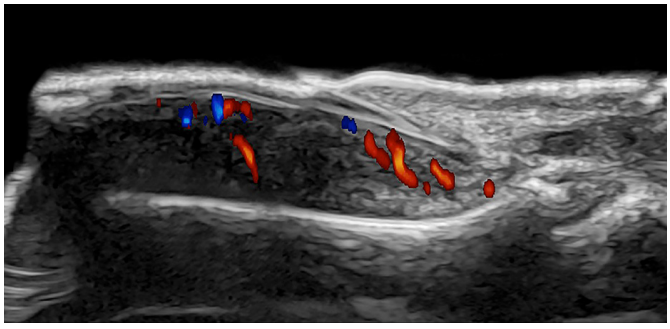

B

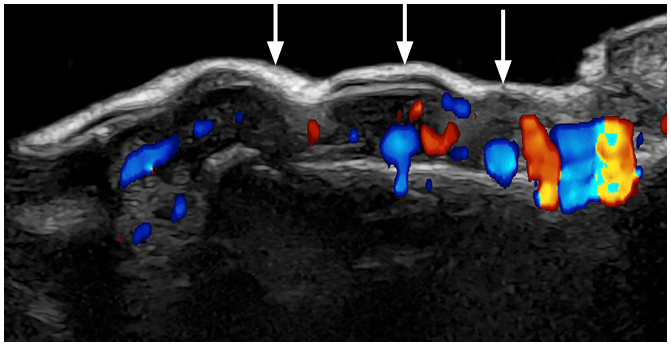

C

Fig. 20. Ultrasound patterns of nail psoriasis (color Doppler; 24 MHz; fingernails).
The hypervascularity of the nail beds should be noticed, as well as the morphological alterations. A–C. On ultrasonography, loss of definition of the ventral plate, hyperechoic deposits in the ventral nail plate (A), thickening and decreased echogenicity of the nail bed (B), and a wavy and thick nail plate (C, arrows) are suggestive of nail psoriasis.

hypovascular to hypervascular in the periphery of the cyst (Fig. 19) [10,11,13,116].

Frequently, there are osteophytes and mild synovitis of the distal interphalangeal and/or interphalangeal joints [10,11,13,116].

Sometimes there are myxoid cysts in multiple fingers, many of them small and subclinical [10,11].

Nail psoriasis

Nail involvement in psoriasis has been linked to a higher frequency of psoriatic arthropathy. This could precede or be concurrent with the cutaneous disease. One of the main clinical problems of nail psoriasis is that it could present challenges for discriminating this entity with onychomycosis and other inflammatory conditions.

On ultrasonography, there are patterns suggestive of nail psoriasis, such as the thickening and decreased echogenicity of the nail bed, hyperechoic deposits in the ventral nail plate, loss of definition of the ventral plate, and a wavy and thick nail plate.

In some cases, there is also epidermal and dermal thickening with decreased dermal echogenicity in the proximal nail fold and hyponychium.

On color Doppler, the vascularity is variable according to the degree of inflammatory activity of the disease, with slow-flow vessels (Fig. 20) [1,10,11,119–130].

Retronychia

Retronychia refers to the posterior embedding of the nail plate, and it is commonly associated with onychomadesis (i.e., fragmentation of the nail plate). This condition can clinically simulate an infection because it can cause erythema and swelling of the proximal nail fold; however, it is an alteration of the location of the nail plate frequently related to trauma.

The ultrasonographic signs of retronychia include the presence of a hypoechoic halo surrounding the proximal part of the nail plate, shortening of the distance between the origin of the nail plate and

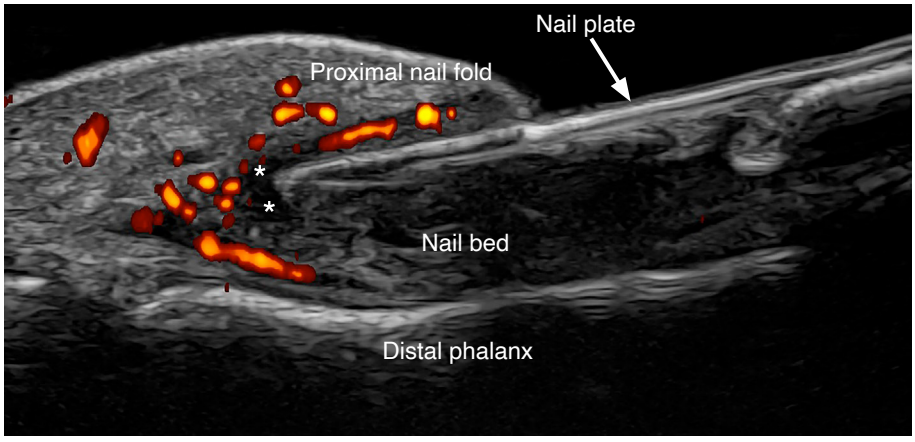

A

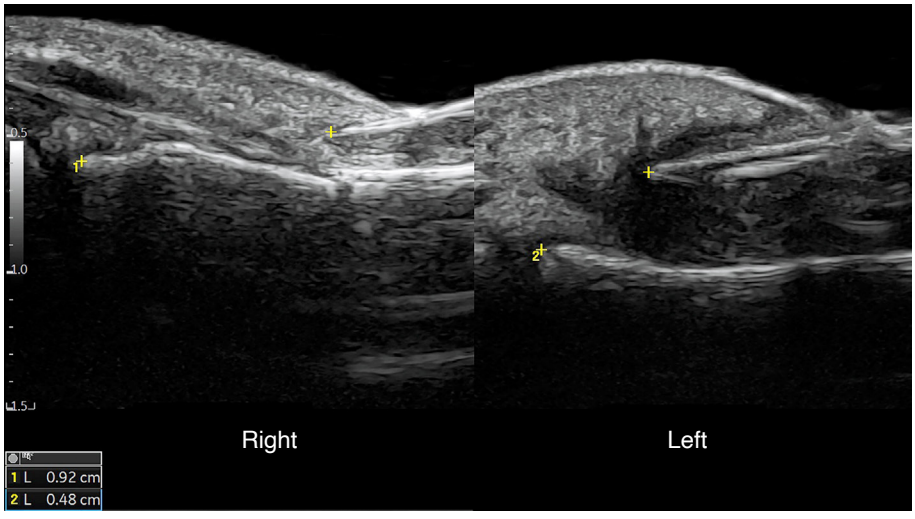

B

Fig. 21. Retronychia at 24 MHz.
A. Power Doppler (left first toe) presents thickening and hypoechogenicity of the nail bed, fragmentation of the proximal nail plate (onychomadesis), thickening and hypoechogenicity of the proximal nail fold. There is a halo sign (*, hypoechoic band) in the periphery of the origin of the nail plate with hypervascularity of the proximal nail fold. B. Grayscale comparative views side-by-side show a decreased distance between the origin of the nail plate and the base of the distal phalanx on the left side (retronychia) versus the right side (4.8 mm vs. 9.2 mm).

the base of the distal phalanx (affected side versus non-affected side), and decreased echogenicity and thickening of the proximal nail fold. In the acute phases, there is hypervascularity of the proximal nail fold and proximal part of the nail bed with low-flow vessels (Fig. 21). Ultrasonographic criteria for diagnosing bilateral retronychia have also been reported in the literature [10,131–133].

Summary

Ultrasonography can be a powerful tool in dermatology to support the diagnosis and the provision of critical anatomical information for common dermatologic entities, which can allow management to be modified.

ORCID: Ximena Wortsman: https://orcid.org/0000-0003-3359-5023

Conflict of Interest

No potential conflict of interest relevant to this article was reported.

References

1. Wortsman X. Top advances in dermatologic ultrasound. J Ultrasound Med 2022;42:521-545.
2. Alfageme F, Wortsman X, Catalano O, Roustan G, Crisan M, Crisan D, et al. European Federation of Societies for Ultrasound in Medicine and Biology (EFSUMB) position statement on dermatologic ultrasound. Ultraschall Med 2021;42:39-47.
3. Almuhanna N, Wortsman X, Wohlmuth-Wieser I, Kinoshita-Ise M, Alhusayen R. Overview of ultrasound imaging applications in dermatology [formula: see text]. J Cutan Med Surg 2021;25:521-529.
4. Catalano O, Varelli C, Sbordone C, Corvino A, De Rosa D, Vallone G, et al. A bump: what to do next? Ultrasound imaging of superficial soft-tissue palpable lesions. J Ultrasound 2020;23:287-300.
5. Mandava A, Ravuri PR, Konathan R. High-resolution ultrasound imaging of cutaneous lesions. Indian J Radiol Imaging 2013;23:269-277.
6. Wortsman X. Common applications of dermatologic sonography. J Ultrasound Med 2012;31:97-111.
7. Wortsman X. Ultrasound in dermatology: why, how, and when? Semin Ultrasound CT MR 2013;34:177-195.
8. Wortsman X, Alfageme F, Roustan G, Arias-Santiago S, Martorell A, Catalano O, et al. Guidelines for performing dermatologic ultrasound examinations by the DERMUS group. J Ultrasound Med 2016;35:577-580.
9. Wortsman X, Carreno L, Ferreira-Wortsman C, Poniachik R, Pizarro K, Morales C, et al. Ultrasound characteristics of the hair follicles and tracts, sebaceous glands, montgomery glands, apocrine glands, and arrector pili muscles. J Ultrasound Med 2019;38:1995-2004.
10. Wortsman X. Atlas of dermatologic ultrasound. New York: Springer International Publishing, 2018.
11. Wortsman X, Jemec GB. Dermatologic ultrasound with clinical and histologic correlations. New York: Springer-Verlag, 2013.
12. Aluja Jaramillo F, Quiasua Mejia DC, Martinez Orduz HM, Gonzalez Ardila C. Nail unit ultrasound: a complete guide of the nail diseases. J Ultrasound 2017;20:181-192.
13. Wortsman X. Concepts, role, and advances on nail imaging. Dermatol Clin 2021;39:337-350.
14. Cataldo-Cerda K, Wortsman X. Dissecting cellulitis of the scalp early diagnosed by color Doppler ultrasound. Int J Trichology 2017;9:147-148.
15. Wortsman X, Guerrero R, Wortsman J. Hair morphology in androgenetic alopecia: sonographic and electron microscopic studies. J Ultrasound Med 2014;33:1265-1272.
16. Wortsman X, Wortsman J. Clinical usefulness of variable-frequency ultrasound in localized lesions of the skin. J Am Acad Dermatol 2010;62:247-256.
17. Al-Khateeb TH, Al-Masri NM, Al-Zoubi F. Cutaneous cysts of the head and neck. J Oral Maxillofac Surg 2009;67:52-57.
18. Bansal AG, Oudsema R, Masseaux JA, Rosenberg HK. US of pediatric superficial masses of the head and neck. Radiographics 2018;38:1239-1263.
19. Huang CC, Ko SF, Huang HY, Ng SH, Lee TY, Lee YW, et al. Epidermal cysts in the superficial soft tissue: sonographic features with an emphasis on the pseudotestis pattern. J Ultrasound Med 2011;30:11-17.
20. Kim HK, Kim SM, Lee SH, Racadio JM, Shin MJ. Subcutaneous epidermal inclusion cysts: ultrasound (US) and MR imaging findings. Skeletal Radiol 2011;40:1415-1419.
21. Kim HW, Yoo SY, Oh S, Jeon TY, Kim JH. Ultrasonography of pediatric superficial soft tissue tumors and tumor-like lesions. Korean J Radiol 2020;21:341-355.
22. Rodriguez Bandera AI, Moreno Bonilla G, Feito Rodriguez M, Beato Merino MJ, de Lucas Laguna R. Usefulness of high-frequency ultrasonography in the assessment of cutaneous lesions in children with hematologic malignancies. Pediatr Dermatol 2018;35:e276-e280.
23. Rodriguez Bandera AI, Sebaratnam DF, Feito Rodriguez M, de Lucas Laguna R. Cutaneous ultrasound and its utility in pediatric dermatology: Part II-Developmental anomalies and vascular lesions. Pediatr Dermatol 2020;37:40-51.
24. Takemura N, Fujii N, Tanaka T. Epidermal cysts: the best surgical method can be determined by ultrasonographic imaging. Clin Exp Dermatol 2007;32:445-447.
25. Wortsman X. Sonography of dermatologic emergencies. J Ultrasound Med 2017;36:1905-1914.
26. Wortsman X. Why, how, and when to use color Doppler ultrasound for improving precision in the diagnosis, assessment of severity and

activity in morphea. J Scleroderma Relat Disord 2019;4:28-34.
27. Wortsman X. Practical applications of ultrasound in dermatology. Clin Dermatol 2021;39:605-623.
28. Zhang Q, Huang Y. Ultrasound-guided sclerotherapy for recurrent epidermoid cyst: a case report. Dermatol Ther 2021;34:e14552.
29. Roche NA, Monstrey SJ, Matton GE. Pilomatricoma in children: common but often misdiagnosed. Acta Chir Belg 2010;110:250-254.
30. Choo HJ, Lee SJ, Lee YH, Lee JH, Oh M, Kim MH, et al. Pilomatricomas: the diagnostic value of ultrasound. Skeletal Radiol 2010;39:243-250.
31. Hassanein AH, Alomari AI, Schmidt BA, Greene AK. Pilomatrixoma imitating infantile hemangioma. J Craniofac Surg 2011;22:734-736.
32. Hwang JY, Lee SW, Lee SM. The common ultrasonographic features of pilomatricoma. J Ultrasound Med 2005;24:1397-1402.
33. Lim HW, Im SA, Lim GY, Park HJ, Lee H, Sung MS, et al. Pilomatricomas in children: imaging characteristics with pathologic correlation. Pediatr Radiol 2007;37:549-555.
34. Lin SF, Xu SH, Xie ZL. Calcifying epithelioma of malherbe (Pilomatrixoma): clinical and sonographic features. J Clin Ultrasound 2018;46:3-7.
35. Pelizzari M, Giovo ME, Innocente N, Perez R. Ultrasound findings in 156 children with 169 pilomatricomas. Pediatr Radiol 2021;51:2038-2046.
36. Wortsman X, Wortsman J, Arellano J, Oroz J, Giugliano C, Benavides MI, et al. Pilomatrixomas presenting as vascular tumors on color Doppler ultrasound. J Pediatr Surg 2010;45:2094-2098.
37. Garcia C, Wortsman X, Bazaes-Nunez D, Pelizzari M, Gonzalez S, Cossio ML, et al. Skin sonography in children: a review. Pediatr Radiol 2022;52:1687-1705.
38. Wortsman X. Atlas of dermatologic ultrasound. New York: Springer, 2018.
39. MacFarlane D, Shah K, Wysong A, Wortsman X, Humphreys TR. The role of imaging in the management of patients with nonmelanoma skin cancer: diagnostic modalities and applications. J Am Acad Dermatol 2017;76:579-588.
40. Wortsman X. Sonography of facial cutaneous basal cell carcinoma: a first-line imaging technique. J Ultrasound Med 2013;32:567-572.
41. Catalano O. Critical analysis of the ultrasonographic criteria for diagnosing lymph node metastasis in patients with cutaneous melanoma: a systematic review. J Ultrasound Med 2011;30:547-560.
42. Catalano O, Caraco C, Mozzillo N, Siani A. Locoregional spread of cutaneous melanoma: sonography findings. AJR Am J Roentgenol 2010;194:735-745.
43. Catalano O, Roldan FA, Varelli C, Bard R, Corvino A, Wortsman X. Skin cancer: findings and role of high-resolution ultrasound. J Ultrasound 2019;22:423-431.
44. Catalano O, Voit C, Sandomenico F, Mandato Y, Petrillo M, Franco R, et al. Previously reported sonographic appearances of regional melanoma metastases are not likely due to necrosis. J Ultrasound Med 2011;30:1041-1049.
45. Khlebnikova AN, Molochkov VA, Selezneva EV, Belova LA, Bezugly A, Molochkov AV. Ultrasonographic features of superficial and nodular basal cell carcinoma. Med Ultrason 2018;20:475-479.
46. Kim HJ, Lee SJ, Lee JH, Shin SH, Xu H, Yang I, et al. Usefulness of ultrasonography in determining the surgical excision margin in non-melanocytic skin cancer: a comparative analysis of preoperative ultrasonography and postoperative histopathology. Medicine (Baltimore) 2020;99:e23789.
47. Lassau N, Spatz A, Avril MF, Tardivon A, Margulis A, Mamelle G, et al. Value of high-frequency US for preoperative assessment of skin tumors. Radiographics 1997;17:1559-1565.
48. Wortsman X, Vergara P, Castro A, Saavedra D, Bobadilla F, Sazunic I, et al. Ultrasound as predictor of histologic subtypes linked to recurrence in basal cell carcinoma of the skin. J Eur Acad Dermatol Venereol 2015;29:702-707.
49. Crisan M, Crisan D, Sannino G, Lupsor M, Badea R, Amzica F. Ultrasonographic staging of cutaneous malignant tumors: an ultrasonographic depth index. Arch Dermatol Res 2013;305:305-313.
50. Crisan D, Wortsman X, Alfageme F, Catalano O, Badea A, Scharffetter-Kochanek K, et al. Ultrasonography in dermatologic surgery: revealing the unseen for improved surgical planning. J Dtsch Dermatol Ges 2022;20:913-926.
51. Wortsman X. Sonography of the primary cutaneous melanoma: a review. Radiol Res Pract 2012;2012:814396.
52. Burkes SA, Adams DM, Hammill AM, Chute C, Eaton KP, Welge JA, et al. Skin imaging modalities quantify progression and stage of infantile haemangiomas. Br J Dermatol 2015;173:838-841.
53. Canty KM, Horii KA, Ahmad H, Lowe LH, Nopper AJ. Multiple cutaneous and hepatic hemangiomas in infants. South Med J 2014;107:159-164.
54. Ding A, Gong X, Li J, Xiong P. Role of ultrasound in diagnosis and differential diagnosis of deep infantile hemangioma and venous malformation. J Vasc Surg Venous Lymphat Disord 2019;7:715-723.
55. Kutz AM, Aranibar L, Lobos N, Wortsman X. Color Doppler ultrasound follow-up of infantile hemangiomas and peripheral vascularity in patients treated with propranolol. Pediatr Dermatol 2015;32:468-475.
56. McNab M, Garcia C, Tabak D, Aranibar L, Castro A, Wortsman X. Subclinical ultrasound characteristics of infantile hemangiomas that may potentially affect involution. J Ultrasound Med 2021;40:1125-1130.
57. Rodriguez Bandera AI, Sebaratnam DF, Wargon O, Wong LF. Infantile hemangioma. Part 1: Epidemiology, pathogenesis, clinical presentation and assessment. J Am Acad Dermatol 2021;85:1379-1392.
58. Rotter A, Samorano LP, de Oliveira Labinas GH, Alvarenga JG,

Rivitti-Machado MC, Bouer M, et al. Ultrasonography as an objective tool for assessment of infantile hemangioma treatment with propranolol. Int J Dermatol 2017;56:190-194.
59. Sebaratnam DF, Rodriguez Bandera AL, Wong LF, Wargon O. Infantile hemangioma. Part 2: Management. J Am Acad Dermatol 2021;85:1395-1404.
60. Jemec GB. Clinical practice: hidradenitis suppurativa. N Engl J Med 2012;366:158-164.
61. Saunte DM, Jemec GB. Hidradenitis suppurativa: advances in diagnosis and treatment. JAMA 2017;318:2019-2032.
62. Wortsman X. Diagnosis and treatment of hidradenitis suppurativa. JAMA 2018;319:1617-1618.
63. Wortsman X. Strong validation of ultrasound as an imaging biomarker in hidradenitis suppurativa. Br J Dermatol 2021;184:591-592.
64. Wortsman X. Color Doppler ultrasound: a standard of care in hidradenitis suppurativa. J Eur Acad Dermatol Venereol 2020;34:e616-e617.
65. Wortsman X, Moreno C, Soto R, Arellano J, Pezo C, Wortsman J. Ultrasound in-depth characterization and staging of hidradenitis suppurativa. Dermatol Surg 2013;39:1835-1842.
66. Reyes-Baraona F, Herane MI, Wortsman X, Figueroa A, Garcia-Huidobro I, Giesen L, et al. Chilean clinical guideline for the management of hidradenitis suppurativa: executive summary. Rev Med Chil 2021;149:1620-1635.
67. Lacarrubba F, Dini V, Napolitano M, Venturini M, Caposiena Caro DR, Molinelli E, et al. Ultrasonography in the pathway to an optimal standard of care of hidradenitis suppurativa: the Italian Ultrasound Working Group experience. J Eur Acad Dermatol Venereol 2019;33 Suppl 6:10-14.
68. Lacarrubba F, Musumeci ML, Martorell A, Palmucci S, Petrillo G, Micali G. Role of the imaging techniques in the diagnosis and staging of hidradenitis suppurativa. G Ital Dermatol Venereol 2018;153:20-25.
69. Loo CH, Tan WC, Tang JJ, Khor YH, Manikam MT, Low DE, et al. The clinical, biochemical, and ultrasonographic characteristics of patients with hidradenitis suppurativa in Northern Peninsular Malaysia: a multicenter study. Int J Dermatol 2018;57:1454-1463.
70. Lyons AB, Narla S, Kohli I, Zubair R, Nahhas AF, Braunberger TL, et al. Assessment of inter-rater reliability of clinical hidradenitis suppurativa outcome measures using ultrasonography. Clin Exp Dermatol 2022;47:319-324.
71. Lyons AB, Zubair R, Kohli I, Hamzavi IH. Preoperative ultrasound for evaluation of hidradenitis suppurativa. Dermatol Surg 2019;45:294-296.
72. Marasca C, Marasca D, Megna M, Annunziata MC, Fabbrocini G. Ultrasound: an indispensable tool to evaluate the outcome of surgical approaches in patients affected by hidradenitis suppurativa. J Eur Acad Dermatol Venereol 2020;34:e413-e414.
73. Martorell A, Alfageme Roldan F, Vilarrasa Rull E, Ruiz-Villaverde R, Romani De Gabriel J, Garcia Martinez F, et al. Ultrasound as a diagnostic and management tool in hidradenitis suppurativa patients: a multicentre study. J Eur Acad Dermatol Venereol 2019;33:2137-2142.
74. Martorell A, Giovanardi G, Gomez-Palencia P, Sanz-Motilva V. Defining fistular patterns in hidradenitis suppurativa: impact on the management. Dermatol Surg 2019;45:1237-1244.
75. Martorell A, Wortsman X, Alfageme F, Roustan G, Arias-Santiago S, Catalano O, et al. Ultrasound evaluation as a complementary test in hidradenitis suppurativa: proposal of a standarized report. Dermatol Surg 2017;43:1065-1073.
76. Nguyen TV, Damiani G, Orenstein LA, Hamzavi I, Jemec GB. Hidradenitis suppurativa: an update on epidemiology, phenotypes, diagnosis, pathogenesis, comorbidities and quality of life. J Eur Acad Dermatol Venereol 2021;35:50-61.
77. Ovadja ZN, Schuit MM, van der Horst C, Lapid O. Inter- and intrarater reliability of Hurley staging for hidradenitis suppurativa. Br J Dermatol 2019;181:344-349.
78. Salvador-Rodriguez L, Arias-Santiago S, Molina-Leyva A. Ultrasound-assisted intralesional corticosteroid infiltrations for patients with hidradenitis suppurativa. Sci Rep 2020;10:13363.
79. Wortsman X, Calderon P, Castro A. Seventy-MHz ultrasound detection of early signs linked to the severity, patterns of keratin fragmentation, and mechanisms of generation of collections and tunnels in hidradenitis suppurativa. J Ultrasound Med 2020;39:845-857.
80. Wortsman X, Castro A, Figueroa A. Color Doppler ultrasound assessment of morphology and types of fistulous tracts in hidradenitis suppurativa (HS). J Am Acad Dermatol 2016;75:760-767.
81. Wortsman X, Castro A, Morales C, Franco C, Figueroa A. Sonographic comparison of morphologic characteristics between pilonidal cysts and hidradenitis suppurativa. J Ultrasound Med 2017;36:2403-2418.
82. Wortsman X, Jemec G. A 3D ultrasound study of sinus tract formation in hidradenitis suppurativa. Dermatol Online J 2013;19:18564.
83. Wortsman X, Jemec GB. Real-time compound imaging ultrasound of hidradenitis suppurativa. Dermatol Surg 2007;33:1340-1342.
84. Wortsman X, Kohli I. Imaging technique in hidradenitis suppurativa and comorbidities. In: Shi V, Hsiao J, Lowes MA, Hamzavi I, eds. A comprehensive guide to hidradenitis suppurativa. Philadelphia, PA: Elsevier, 2021;45-61.
85. Wortsman X, Rodriguez C, Lobos C, Eguiguren G, Molina MT. Ultrasound diagnosis and staging in pediatric hidradenitis suppurativa. Pediatr Dermatol 2016;33:e260-e264.
86. Wortsman X, Wortsman J. Ultrasound detection of retained hair tracts in hidradenitis suppurativa. Dermatol Surg 2015;41:867-869.
87. Zarchi K, Jemec GB. The role of ultrasound in severity assessment in hidradenitis suppurativa. Dermatol Surg 2014;40:592.

88. Zarchi K, Yazdanyar N, Yazdanyar S, Wortsman X, Jemec GB. Pain and inflammation in hidradenitis suppurativa correspond to morphological changes identified by high-frequency ultrasound. J Eur Acad Dermatol Venereol 2015;29:527-532.
89. Wortsman X, Wortsman J, Sazunic I, Carreno L. Activity assessment in morphea using color Doppler ultrasound. J Am Acad Dermatol 2011;65:942-948.
90. Araneda-Ortega P, Poblete-Villacorta MJ, Munoz-Lopez C, Vera-Kellet C, Wortsman X. Morphea after liposuction ultrasonography. J Ultrasound Med 2022;41:2629-2635.
91. Fett NM. Morphea (localized scleroderma). JAMA Dermatol 2013;149:1124.
92. Marti-Marti I, Morgado-Carrasco D, Podlipnik S, Rizo-Potau D, Bosch-Amate X, Lledo GM, et al. Usefulness of high-frequency ultrasonography in the evaluation and monitoring of sclerosing dermatoses: a cohort study. Clin Exp Dermatol 2022;47:351-358.
93. Peterson LS, Nelson AM, Su WP. Classification of morphea (localized scleroderma). Mayo Clin Proc 1995;70:1068-1076.
94. Polanska A, Danczak-Pazdrowska A, Olek-Hrab K, Osmola-Mankowska A, Bowszyc-Dmochowska M, Zaba R, et al. High-frequency ultrasonography-new non-invasive method in assessment of skin lymphomas. Skin Res Technol 2018;24:517-521.
95. Porta F, Kaloudi O, Garzitto A, Prignano F, Nacci F, Falcini F, et al. High frequency ultrasound can detect improvement of lesions in juvenile localized scleroderma. Mod Rheumatol 2014;24:869-873.
96. Vera-Kellet C, Meza-Romero R, Moll-Manzur C, Ramirez-Cornejo C, Wortsman X. Low effectiveness of methotrexate in the management of localised scleroderma (morphea) based on an ultrasound activity score. Eur J Dermatol 2021;31:813-821.
97. Quezada-Gaon N, Wortsman X. Ultrasound-guided hyaluronidase injection in cosmetic complications. J Eur Acad Dermatol Venereol 2016;30:e39-e40.
98. Schelke LW, Cassuto D, Velthuis P, Wortsman X. Nomenclature proposal for the sonographic description and reporting of soft tissue fillers. J Cosmet Dermatol 2020;19:282-288.
99. Schelke LW, Van Den Elzen HJ, Erkamp PP, Neumann HA. Use of ultrasound to provide overall information on facial fillers and surrounding tissue. Dermatol Surg 2010;36 Suppl 3:1843-1851.
100. Schelke LW, Velthuis P, Kadouch J, Swift A. Early ultrasound for diagnosis and treatment of vascular adverse events with hyaluronic acid fillers. J Am Acad Dermatol 2023;88:79-85.
101. Wortsman X. Identification and complications of cosmetic fillers: sonography first. J Ultrasound Med 2015;34:1163-1172.
102. Wortsman X, Quezada N. Ultrasound morphology of polycaprolactone filler. J Ultrasound Med 2017;36:2611-2615.
103. Wortsman X, Wortsman J. Polyacrylamide fillers on skin ultrasound. J Eur Acad Dermatol Venereol 2012;26:660-661.
104. Wortsman X, Wortsman J, Orlandi C, Cardenas G, Sazunic I, Jemec GB. Ultrasound detection and identification of cosmetic fillers in the skin. J Eur Acad Dermatol Venereol 2012;26:292-301.
105. Young SR, Bolton PA, Downie J. Use of high-frequency ultrasound in the assessment of injectable dermal fillers. Skin Res Technol 2008;14:320-323.
106. Perez-Perez L, Garcia-Gavin J, Wortsman X, Santos-Briz A. Delayed adverse subcutaneous reaction to a new family of hyaluronic acid dermal fillers with clinical, ultrasound, and histologic correlation. Dermatol Surg 2017;43:605-608.
107. Romani J, Giavedoni P, Roe E, Vidal D, Luelmo J, Wortsman X. Inter- and intra-rater agreement of dermatologic ultrasound for the diagnosis of lobular and septal panniculitis. J Ultrasound Med 2020;39:107-112.
108. Woodward J, Khan T, Martin J. Facial filler complications. Facial Plast Surg Clin North Am 2015;23:447-458.
109. Wortsman X, Moll-Manzur C, Ramirez-Cornejo C, Alfaro-Sepulveda D, Mellado-Francisco G, Rezende J, et al. Ultrasonographic subclinical signs of inflammation of the lacrimal, parotid, and submandibular glands in users of cosmetic fillers. J Ultrasound Med 2021;40:2377-2389.
110. Baek HJ, Lee SJ, Cho KH, Choo HJ, Lee SM, Lee YH, et al. Subungual tumors: clinicopathologic correlation with US and MR imaging findings. Radiographics 2010;30:1621-1636.
111. Chen L, Gao YH, Chen J, Yao YJ, Wang R, Yu Q, et al. Diagnosis of subungual glomus tumors with 18 MHz ultrasound and CDFI. Sci Rep 2020;10:17848.
112. Chiang YP, Hsu CY, Lien WC, Chang YJ. Ultrasonographic appearance of subungual glomus tumors. J Clin Ultrasound 2014;42:336-340.
113. Karegowda LH, Shenoy PM, Maddukuri SB, Kyalakond H. Importance of radiological imaging in a case of subungual glomus tumour. BMJ Case Rep 2014;2014:bcr2014205649.
114. Wortsman X, Jemec GB. Ultrasound imaging of nails. Dermatol Clin 2006;24:323-328.
115. Wortsman X, Jemec GB. Role of high-variable frequency ultrasound in preoperative diagnosis of glomus tumors: a pilot study. Am J Clin Dermatol 2009;10:23-27.
116. Wortsman X, Wortsman J, Soto R, Saavedra T, Honeyman J, Sazunic I, et al. Benign tumors and pseudotumors of the nail: a novel application of sonography. J Ultrasound Med 2010;29:803-816.
117. Peruilh-Bagolini L, Dossi MT, Wortsman X, Montero T. Pigmented onychomatricoma: a clinical simulator that could not mislead ultrasound. Acta Biomed 2021;92:e2021158.
118. Soto R, Wortsman X, Corredoira Y. Onychomatricoma: clinical and sonographic findings. Arch Dermatol 2009;145:1461-1462.
119. Castellanos-Gonzalez M, Joven BE, Sanchez J, Andres-Esteban EM, Vanaclocha-Sebastian F, Romero PO, et al. Nail involvement can predict enthesopathy in patients with psoriasis. J Dtsch Dermatol Ges 2016;14:1102-1107.

120. Fernandes L, Amaral W, Evangelista P, Ribeiro AM, Mendonca J. Ultrasonography and Doppler in patients with psoriasis and psoriatic arthritis. Eur J Dermatol 2019;29:565-566.
121. Griffiths CE, Barker JN. Pathogenesis and clinical features of psoriasis. Lancet 2007;370:263-271.
122. Gutierrez M, De Angelis R, Bernardini ML, Filippucci E, Goteri G, Brandozzi G, et al. Clinical, power Doppler sonography and histological assessment of the psoriatic plaque: short-term monitoring in patients treated with etanercept. Br J Dermatol 2011;164:33-37.
123. Gutierrez M, Di Geso L, Salaffi F, Bertolazzi C, Tardella M, Filosa G, et al. Development of a preliminary US power Doppler composite score for monitoring treatment in PsA. Rheumatology (Oxford) 2012;51:1261-1268.
124. Gutierrez M, Filippucci E, De Angelis R, Filosa G, Kane D, Grassi W. A sonographic spectrum of psoriatic arthritis: "the five targets". Clin Rheumatol 2010;29:133-142.
125. Gutierrez M, Kaeley GS, Bertolazzi C, Pineda C. State of the art of ultrasound in the assessment of psoriasis and psoriatic arthritis. Expert Rev Clin Immunol 2017;13:439-447.
126. Gutierrez M, Wortsman X, Filippucci E, De Angelis R, Filosa G, Grassi W. High-frequency sonography in the evaluation of psoriasis: nail and skin involvement. J Ultrasound Med 2009;28:1569-1574.
127. Gutierrez-Manjarrez J, Gutierrez M, Bertolazzi C, Afaro-Rodriguez A, Pineda C. Ultrasound as a useful tool to integrate the clinical assessment of nail involvement in psoriatic arthritis. Reumatologia 2018;56:42-44.
128. Michelsen B, Diamantopoulos AP, Hammer HB, Soldal DM, Kavanaugh A, Haugeberg G. Ultrasonographic evaluation in psoriatic arthritis is of major importance in evaluating disease activity. Ann Rheum Dis 2016;75:2108-2113.
129. Naredo E, Moller I, de Miguel E, Batlle-Gualda E, Acebes C, Brito E, et al. High prevalence of ultrasonographic synovitis and enthesopathy in patients with psoriasis without psoriatic arthritis: a prospective case-control study. Rheumatology (Oxford) 2011;50:1838-1848.
130. Sandobal C, Carbo E, Iribas J, Roverano S, Paira S. Ultrasound nail imaging on patients with psoriasis and psoriatic arthritis compared with rheumatoid arthritis and control subjects. J Clin Rheumatol 2014;20:21-24.
131. Fernandez J, Reyes-Baraona F, Wortsman X. Ultrasonographic criteria for diagnosing unilateral and bilateral retronychia. J Ultrasound Med 2018;37:1201-1209.
132. Wortsman X, Calderon P, Baran R. Finger retronychias detected early by 3D ultrasound examination. J Eur Acad Dermatol Venereol 2012;26:254-256.
133. Wortsman X, Wortsman J, Guerrero R, Soto R, Baran R. Anatomical changes in retronychia and onychomadesis detected using ultrasound. Dermatol Surg 2010;36:1615-1620.